https://doi.org/10.5194/egusphere-2023-1498
Preprint. Discussion started: 11 July 2023

The fate of fixed nitrogen in Santa Barbara Basin sediments during seasonal anoxia

Xuefeng Peng[1,2,3], David J. Yousavich[4], Annie Bourbonnais[1], Frank Wenzhöfer[5,6,7], Felix Janssen[5,6], Tina Treude[4,8] and David L. Valentine[2,3]

[1]School of Earth, Ocean and Environment, University of South Carolina, 701 Sumter Street, Columbia, SC, USA

[2]Marine Science Institute, University of California, Santa Barbara, CA, USA

[3]Department of Earth Science, 1006 Webb Hall, University of California, Santa Barbara, CA, USA

[4]Department of Earth, Planetary, and Space Sciences, University of California Los Angeles, 595 Charles E. Young Drive East, Los Angeles, CA, USA

[5]HGF-MPG Joint Research Group for Deep-Sea Ecology and Technology, Alfred-Wegener-Institute, Helmholtz Centre for Polar and Marine Research, Am Handelshafen 12, Bremerhaven, Germany

[6]Max Planck Institute for Marine Microbiology, Celsiusstrasse 1, Bremen, Germany

[7]Department of Biology, DIAS, Nordcee and HADAL Centres, University of Southern Denmark, Odense M, Denmark

[8]Department of Atmospheric and Oceanic Sciences, University of California Los Angeles, Math Science Building, 520 Portola Plaza, Los Angeles, CA, USA.

Correspondence to: Xuefeng Peng (xpeng@seoe.sc.edu) and David L. Valentine (valentine@ucsb.edu)

Abstract.

Despite long-standing interests in the biogeochemistry of the Santa Barbara Basin (SBB), there are no direct rate measurements of different nitrogen transformation processes. We investigated benthic nitrogen cycling using in-situ incubations with $^{15}NO_3^-$ addition and quantified the rates of total nitrate (NO_3^-) uptake, denitrification, anaerobic ammonia oxidation (anammox), N_2O production, and dissimilatory nitrate reduction to ammonia (DNRA). Denitrification was the dominant NO_3^- reduction process, while anammox contributed 0 - 27% to total NO_3^- reduction. DNRA accounted for less than half of NO_3^- reduction except at the deepest station at the center of the SBB where NO_3^- concentration was lowest. NO_3^- availability and sediment total organic carbon content appeared to be two key controls on the relative importance of DNRA. The negative correlation between NO_3^- availability and the relative importance of DNRA suggests a negative feedback loop that potentially contributes to stabilizing the fixed N budget in the SBB. Nitrous oxide (N_2O) production as a fraction of total NO_3^- reduction ranged from 0.2% to 1.5%, which was higher than previous reports from nearby borderland basins. A large fraction of NO_3^- uptake was unaccounted for by NO_3^- reduction processes, suggesting that intracellular storage may play an important role. Our results indicate that the SBB acts as a strong sink for fixed nitrogen and potentially a net source of N_2O to the water column.

https://doi.org/10.5194/egusphere-2023-1498
Preprint. Discussion started: 11 July 2023

1 Introduction

Oxygen minimum zones (OMZs) in the world's ocean, whether they are formed naturally or induced by human activities, have been expanding in the past century (Horak et al., 2016; Oschlies et al., 2017; Stramma et al., 2008). As oxygen (O_2) concentration is one of the key controls on biogeochemical processes, including nitrogen (N) cycling, N biogeochemistry in OMZs has been extensively studied (Paulmier and Ruiz-Pino, 2009; Zehr, 2009). Denitrification, the reduction of nitrate (NO_3^-) to dinitrogen gas (N_2), and anaerobic ammonia oxidation (anammox), where nitrite (NO_2^-) and ammonium (NH_4^+) are converted into N_2 by comproportionation are two major sinks of the oceanic fixed N budget (Gruber, 2008). These two processes are inhibited by the presence of O_2 and sulfide, and their rates are sensitive to O_2 at nanomolar concentrations (Dalsgaard et al., 2014; Joye and Hollibaugh, 1995; Caffrey et al., 2019). Because the last step of the sequential reduction of NO_3^- during denitrification, N_2O reduction, is the most sensitive to O_2 (Zumft, 1997), the production of nitrous oxide (N_2O) as a byproduct of denitrification is usually elevated under hypoxic conditions, i.e., in the presence of O_2 (Firestone et al., 1980; Ji et al., 2015). Additionally, nitrification, i.e., the oxidation of NH_4^+ and subsequently NO_2^- is another major source of N_2O in the ocean (Elkins et al., 1978), and the relative yield of N_2O from nitrification is high under low-O_2 conditions (<4 µM) (Ji et al., 2018). Under O_2 limitation, dissimilatory nitrate reduction to ammonia (DNRA) coupled to organic matter degradation is another important process that results in fixed N retention instead of removal (Burgin and Hamilton, 2007). When viewed as competing processes, DNRA is favored over denitrification under NO_3^--limited conditions where electron donors are in excess (Tiedje et al., 1983). Additionally, under sulfidic conditions, autotrophic DNRA coupled to sulfide oxidation can become a dominant pathway for NO_3^- reduction (Shao et al., 2011, p.201).

The Santa Barbara Basin (SBB) is one of the borderland basins off the southern part of the coast of California and characterized by high export production (Thunell, 1998). Because the bottom water (maximum depth 586 m) in the SBB is separated from the area outside the basin by relatively shallow sills on the eastern end (~200 m deep) and the western end (~475 m deep), O_2 concentrations at the basin's bottom is generally low and usually fluctuates between 1 and 30 µM (Bograd et al., 2002;

Goericke et al., 2015; Reimers et al., 1990; Sholkovitz and Gieskes, 1971; Myhre et al., 2018). During upwelling seasons (winter and spring), water is advected from outside the basin and replenishes bottom water O_2 in the SBB. However, high export production fuels O_2 demand that maintains low O_2 levels within the basin at depths below the deeper sill (Thunell, 1998). As a consequence, anoxia develops at the bottom of the SBB until the next upwelling event (Goericke et al., 2015).

Using water column NO_3^- concentration data collected in the SBB by the California Cooperative Oceanic Fisheries Investigations (CalCOFI) along longitudinal transects (Koslow et al., 2010), Valentine et al. (2016) estimated the benthic NO_3^- uptake rate to be as high as 11.7 mmol m^{-2} d^{-1}, which was one of the highest rates ever reported. However, the fate of the NO_3^- in the sediments remains unclear as there are no direct rate measurements of N cycling processes in the SBB. Indirect estimates using analysis of stable isotopes of water column NO_3^- suggests that benthic denitrification accounts for > 75% of NO_3^- loss in the SBB, and the rates of benthic denitrification were estimated to be the highest among borderland basins in the eastern tropical North Pacific (Sigman et al., 2003). With respect to N_2O, these other borderland basins are considered to be a weak sink (Townsend-Small et al., 2014). As the SBB stands out in terms of denitrification, it may be expected that SBB benthic cycling of N_2O is also unique. Benthic anammox is expected to occur in the SBB (Prokopenko et al., 2006), but the relative contribution of denitrification and anammox to N_2 production has not been assessed.

To decipher the fate of NO_3^- taken up by SBB sediments, we performed in-situ incubations using benthic flux chambers with added $^{15}NO_3^-$ along the bottom slope traversing north-south across the deeper portion of the SBB. By calculating the rates of N_2 production by denitrification and anammox, total N_2O production, and DNRA, we assess the overall rates of NO_3^- uptake and reduction rates. Accompanying geochemical data are used to explore the controls on the relative importance of NO_3^- retention via DNRA.

2 Materials and Methods

2.1 In situ incubations with benthic flux chambers

Remotely operated vehicle (ROV) Jason deployed automated benthic flux chambers (BFC) and conducted sediment push coring at seven stations (Fig. 1) in the SBB along a southern and a northern depth and O_2 gradient originating from the depocenter in the deepest point of the basin (Table 1). Station depth, latitude, and longitude were automatically generated by the Jason data processor using navigation data derived from the Doppler Velocity Log system and the ultrashort baseline positioning system. Bottom water O_2 concentration was determined using a Type 4831 O_2 optode sensor (Aanderaa Data Instruments AS, Bergen, NO) on the ROV and calibrated against Winkler titration measurements of sweater collected from Niskin bottles (Qin et al., 2022). Bottom water was collected using Niskin bottles and stored frozen at -30°C until lab analysis for nitrate (NO_3^-) concentration following the spectrophotometric method described by (García-Robledo et al., 2014).

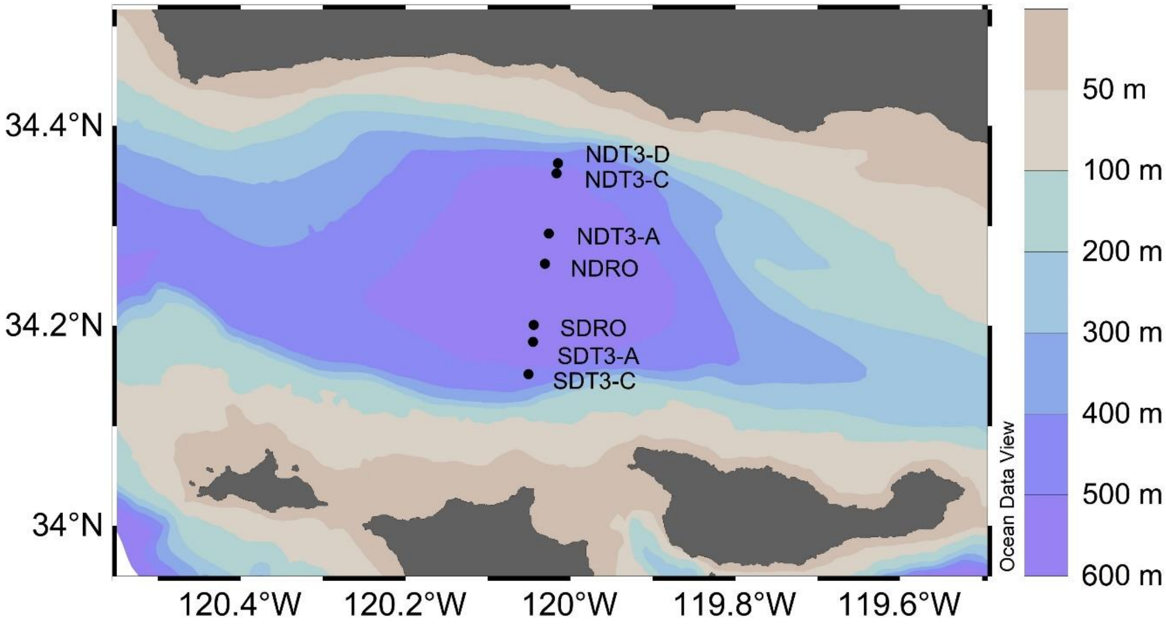

Figure 1. Sampling stations in the Santa Barbara Basin. The color contours show bathymetry data from the General Bathymetric Chart of the Oceans at 30 arc seconds resolution (Becker et al., 2009) visualized in Ocean Data View v5.6.2 (Schlitzer, 2002).

Table 1. Sampling date, latitude, longitude, depth, bottom water concentrations of oxygen and nitrate, chamber volume, total organic carbon (TOC) and nitrogen (TON), and C:N ratio of organic matter in the top 2 cm of the sediment (by dry weight %) at the seven sampling stations in the Santa Barbara Basin. Oxygen concentrations below detection limit of the Type 4831 (Aanderaa Data Instruments AS, Bergen, NO) oxygen optode sensor (3 µM) and the Winkler titration method (1 µM) is denoted by "bdl". Note that oxygen concentrations in the bottom water at NDRO and SDRO were confirmed to be zero through additional analytical methods (see Yousavich et al. 2023).

Station	**NDT3-D**	**NDT3-C**	**NDT3-A**	**NDRO**	**SDRO**	**SDT3-A**	**SDT3-C**
Date	7 Nov 2019	6 Nov 2019	4 Nov 2019	4 Nov 2019	3 Nov 2019	2 Nov 2019	8 Nov 2019
Latitude	34.363°N	34.353°N	34.292°N	34.261°N	34.201°N	34.184°N	34.152°N
Longitude	120.015°W	120.016°W	120.026°W	120.031°W	120.045°W	120.047°W	120.050°W
Depth (m)	447	498	572	580	586	571	494
Chamber ID	BFC1	BFC1	BFC1	BFC3	BFC1	BFC1	BFC1
Chamber volume (L)	3.435	4.321	3.925	3.791	2.416	2.719	3.092
Bottom water O_2 (µM)	8.7	5.2	9.2	bdl	bdl	bdl	3.1
Chamber O_2 (µM) at T_0	8.0	6.0	7.5	3.5	3.0	2.5	6.5
Chamber O_2 (µM) at T_{end}	7.0	6.5	8.5	10.0	1.0	1.7	6.5
Nitrate (µM)	27.3	26.0	24.4	18.5	9.9	20.4	16.3
TOC (%)	4.1%	4.6%	5.9%	5.7%	6.2%	6.8%	5.3%
TON (%)	0.5%	0.5%	0.7%	0.7%	0.8%	0.9%	0.6%
C:N ratio	8.85	8.65	8.11	8.04	7.95	7.53	8.25

Sediment samples for total organic carbon (TOC) and total organic nitrogen (TON) analyses were subsampled from push cores (polycarbonate, 30.5 cm length, 6.35 cm inner diameter) retrieved by ROV Jason that were sectioned in 1-cm increments up to 10 cm followed by 2-cm increments below 10 cm (Yousavich et al., 2023). Wet sediments were dried for up to 48 hours at 50°C and treated with 6N HCl to dissolve carbonate minerals (Harris et al., 2001). Samples were then washed with ultrapure water and

https://doi.org/10.5194/egusphere-2023-1498
Preprint. Discussion started: 11 July 2023

dried again at 50°C. An aliquot (~10-15 mg) was then packed into individual 8x5 mm pressed tin capsules and analyzed at the University of California Davis stable isotope facility using a PDZ Europa 20-20 isotope ratio mass spectrometer (Sercon Ltd., Cheshire, UK). TOC and TON were calculated based on the sample peak area corrected against a reference material (alfalfa flour). Molar concentrations, obtained from measured TOC and TON (in wt%) were used to calculate carbon-to-nitrogen (C:N) ratios.

The design of the BFCs has been described previously (Vonnahme et al., 2020). In brief, a stirred cylindrical polycarbonate chamber (inner diameter = 19 cm) equipped with conductivity and oxygen sensors in the lid (type 5860 and 4330, respectively, Aanderaa Data Instruments AS, Bergen, NO) was inserted into the sediment to enclose a sediment patch of 284 cm^2 together with 2.5 to 4.5 L of overlying water. The chambers were outfitted with a syringe sampler hosting one injection syringe and six sampling syringes to inject into and take samples from the overlying water at approximately 60-minute intervals. The injection syringe contained 200 µmol of ^{15}N-labeled potassium nitrate (Cambridge Isotopes) dissolved in 50 ml of deionized water. To minimize the introduction of O_2, the ^{15}N-labeled potassium nitrate solution was purged by ultra-high purity helium at 5 ml min^{-1} for 60 minutes prior to be loaded into the injection syringe. The post-injection decrease in salinity in the chamber (as detected by the conductivity sensor) was used to calculate the volume of the benthic flux chamber (Kononets et al., 2021). Depending on the chamber volume, the total concentration of NO_3^- ranged between 50 and 100 µM at the beginning of in-situ incubations. This level of NO_3^- amendment was intended to prevent its depletion before the end of incubations given the potentially high rates of NO_3^- uptake estimated by a previous study (Valentine et al., 2016).

Water samples from the BFC were transferred to evacuated 12-ml vials (Exetainer®, Labco, Lampeter, UK) pre-filled with 0.1 ml of 7 M zinc chloride for preservation. Prior to analysis of the isotopic compositions of N_2 and N_2O, 5 mL sample was replaced with ultra-high purity helium to create a headspace. The concentration and $\delta^{15}N$ of dissolved N_2 and N_2O was determined using a Sercon CryoPrep gas concentration system interfaced to a Sercon 20-20 isotope-ratio mass spectrometer

(IRMS) at the University of California Davis Stable Isotope Facility. The measurement precision was ±0.2 ‰ for $\delta^{15}N$.

Water samples from the benthic flux chambers for analysis of $^{15}NH_4^+$ were filtered through sterile 47-mm syringe filters (0.2 µm pore size) and frozen immediately. The production of $^{15}NH_4^+$ in seawater samples was measured using a method adapted from *Zhang et al.* (2007) and described previously (Peng et al., 2016). In brief, NH_4^+ was first oxidized to NO_2^- using hypobromite (BrO^-) and then reduced to N_2O using an acetic acid-azide working solution (McIlvin and Altabet, 2005; Zhang et al., 2007). The $\delta^{15}N$ of the produced N_2O was determined using an Elementar Americas PrecisION continuous flow, multicollector, isotope-ratio mass spectrometer (CF-MC-IRMS) coupled to a custom-built automated gas extraction and preparation system similar to the system described in McIlvin and Casciotti (2011). Calibration and correction were performed as described in Zhang et al. (2007). The measurement precision was ± 0.2‰ for $\delta^{15}N$. NH_4^+ solutions (10 µM) from a mixture of 99% $^{15}NH_4Cl$ (Cambridge Isotopes) and IAEA standard N1 ($\delta^{15}N$ = 1.2‰) with a final $\delta^{15}N$ of 135‰, 676‰, 1,351‰, 5,404‰, and 10,806‰ were prepared and used as in-house reference standards. The IRMS measurements of these in-house reference standards scaled linearly (R^2 = 0.9996) with their $\delta^{15}N$ values.

2.2 Rate calculations and statistics

Production rates of $^{29}N_2$, $^{30}N_2$, $^{15}NH_4^+$, and total N_2O were calculated from the slope of the concentrations of the respective species at the syringe sampling time points by fitting a linear regression multiplied by the overlying water column volume and divided by the chamber area. The linear regressions excluded the last one or two sampling time points if they clearly deviated from a linear trend compared to the first four or five sampling time points. The rates of N_2 production from denitrification and anammox were calculated following a previously described method (Thamdrup and Dalsgaard, 2002) with modifications to account for coupled DNRA-anammox. The calculation was set up with denitrification rate (R_{DN}) and anammox rate (R_{AMX}) as unknowns:

$$R_{DN} \cdot f_N^2 + R_{AMX} \cdot f_A \cdot f_N = P^{30} \qquad \text{(Eqn. 1)}$$

$$R_{DN} \cdot 2 \cdot f_N \cdot (1 - f_N) + R_{AMX} \cdot [f_A \cdot (1 - f_N) + (1 - f_A) \cdot f_N] = P^{29} \qquad \text{(Eqn. 2)}$$

where P^{29} and P^{30} are the respective production rates of $^{29}N_2$ and $^{30}N_2$ that were calculated from measured concentrations stated above, f_N is the fraction of ^{15}N in the NO_3^- pool and f_A is the fraction of ^{15}N in the NH_4^+ pool. The solution for R_{DN} and R_{AMX} is:

$$R_{DN} = \frac{(f_A + f_N - 2 \cdot f_A \cdot f_N) \cdot P^{30} - f_A \cdot f_N \cdot P^{29}}{f_N^2 \cdot (f_N - f_A)} \qquad \text{(Eqn. 3)}$$

$$R_{AMX} = \frac{f_N \cdot P^{29} - 2 \cdot (1 - f_N) \cdot P^{30}}{f_N \cdot (f_N - f_A)} \qquad \text{(Eqn. 4)}$$

Errors calculated from the linear regression of $^{29}N_2$ and $^{30}N_2$ production rates were propagated to R_{DN} and R_{AMX} following established statistical methods (Deming, 1943). Detection limits of the calculated rates were estimated as double the standard deviation from linear regressions. Depending on the in-situ NO_3^- concentration, the detection limit for total N_2 production from denitrification and anammox ranged between 0.04 and 0.17 mmol m^{-2} d^{-1} and 0.04 and 0.24 mmol m^{-2} d^{-1} (Table S1), respectively. The detection limit for N_2O production ranged between 1.1 and 5.6 µmol m^{-2} d^{-1}. DNRA rates were calculated as the rates of increase in $^{15}NH_4^+$ divided by f^{15}, where f^{15} is the fraction of ^{15}N in the NO_3^- pool. Because part of the produced $^{15}NH_4^+$ would be adsorbed to sediment minerals, the rates of $^{15}NH_4^+$ production were further multiplied by a factor of two (De Brabandere et al., 2015; Laima, 1994). Depending on the in-situ NH_4^+ concentration, the detection limit for total NH_4^+ production rates ranged between 0.01 and 0.07 mmol m^{-2} d^{-1} (Table S1).

3 Results and Discussion

3.1 Interpretation of rate measurements from benthic flux chamber incubations

The use of benthic flux chambers to perform $^{15}NO_3^-$ incubation experiments in situ offers multiple advantages over other techniques such as slurry or whole-core incubations, including minimal disturbance of the sediment, maintenance of in-situ pressure and temperature, and relatively large surface area which can account for spatial heterogeneity (Aller et al., 1998; Hall et al., 2007; Nielsen and Glud, 1996; Robertson et al., 2019). One shortcoming of the tracer incubations with benthic flux chambers in this study is that the diffusion of added $^{15}NO_3^-$ into sediments and the labeled $^{15}NO_3^-$

reduction products out of sediments was unlikely at steady state. $^{15}NO_3^-$ added to the overlying water of the chambers diffuses into sediment porewater where O_2 is depleted within the first few millimeters, sustaining benthic NO_3^- reduction. However, a share of the labeled N-compounds that are produced will diffuse to pore waters in deeper sediment layers and, hence, cannot be detected in samples taken from the overlying waters. O_2 in bottom water (and, therefore, also in pore waters) was depleted (below detection of the Winkler titration method, 1 µM) at the deepest stations SDRO and NDRO (Table 1). The NO_3^- reduction rates measured in our experiments represent only the benthic contribution because the water samples in the six sampling syringes were sub-sampled simultaneously after recovery and no preservative was added inside the sampling syringe to terminate reactions. Therefore, we assume that NO_3^- reduction in the overlying water contributed equally among all six sampling syringes to the production of N_2, N_2O, and NH_4^+, and does not interfere with our rate calculations. Separate water incubations would be needed to determine the rates of NO_3^- reduction in the water column.

To account for NH_4^+ adsorption which could lead to an underestimate of DNRA, we made the assumption that an amount of $^{15}NH_4^+$ that equals the measured increase in the benthic flux chambers is adsorbed to sediment minerals (Hall et al., 2017; Laima, 1994). Although the reported production rates of N_2, N_2O, and NH_4^+ only accounted for the changes apparent in the chamber water column, they may not be underestimates of the actual rates, because the addition of NO_3^- at concentrations that were 1.6 - 6.2 (median = 2.3) times as high as ambient concentrations resulted in NO_3^- uptake rates elevated by a factor of 1.9 - 6.4 (median = 3.8) as compared to those measured in parallel chambers deployed at the same time without any added substrates (Table S2; (Yousavich et al., 2023). While the diffusive loss of NO_3^- to the sediment porewater is expected to account for the stimulated NO_3^- uptake partially, NO_3^- addition also likely stimulated the rates of NO_3^- reduction and intracellular storage. However, it remains unclear whether the accelerated NO_3^- uptake is partitioned between intracellular storage and reduction in the same proportion as under unamended conditions, which would partially depend on the carrying capacity of NO_3^- storage vs. reduction. Therefore, we conservatively interpret the production rates of N_2, N_2O, and NH_4^+ reported here to be on the same order of magnitude as the actual rates, and the relative contribution of different NO_3^- reduction processes to be representative of in-situ conditions.

After all, the reported areal rates only represent benthic processes, which were estimated to account for three quarters of the denitrification in the SBB (Sigman et al., 2003).

O_2 concentrations in the overlying water in most incubations were slightly increasing over the time period of the incubation with an average rate of 0.11 ± 0.44 µmol h^{-1}. The increase is attributed to a release of O_2 from the polycarbonate walls and lids of the chambers that were exposed to air until shortly before deployment. The net increase in O_2 in the overlying water indicates that rates of O_2 provision from the plastics were in most cases higher than the rates of O_2 uptake by the enclosed sediment. A release of O_2 from plastics has been reported by a previous study which showed rates of O_2 provided from polycarbonate to O_2-poor waters were among the highest of all plastics tested (Stevens, 1992). The extent to which the artificial elevation of O_2 levels in the water overlaying the sediment in the chambers may have affected N-transformation pathways and rates will depend on the O_2 sensitivity of the respective processes and the penetration depth of O_2 into the sediment. This effect was likely insignificant in our incubations in the SBB because the rate of O_2 change was minimal compared to ambient O_2 concentrations except for station NDRO (Table 1). We note that at station NDRO, O_2 concentration in the chamber water rose from below detection to 10 µM, which likely resulted in an underestimate of the NO_3^- reduction rates.

3.2 Denitrification was the dominant NO_3^- reduction pathway

On average, N_2 production by denitrification and anammox was dominant over DNRA in this study, accounting for 70.4 ± 16.4% of total NO_3^- reduction (Fig. 2 and Table 2). Total N_2 production rates ranged from 0.89 to 3.60 mmol N m^{-2} d^{-1}, which were lower compared to a previous estimate (~4.5 mmol N m^{-2} d^{-1}) based on NO_3^- stable isotope mass balance calculations for the SBB (Sigman et al., 2003). Nevertheless, the previous estimate includes large uncertainties and the rates calculated from stable isotope mass balance represent signals integrated over multiple seasons (Sigman et al., 2003), whereas our measurements represent snapshots obtained in one season of one year when the bottom water NO_3^- was not depleted. N_2 production rates at seasons more depleted in NO_3^- concentrations in the bottom water compared to our study might more closely resemble rates estimated by Sigman et al.

https://doi.org/10.5194/egusphere-2023-1498
Preprint. Discussion started: 11 July 2023

(2003). Season-resolving studies are needed in the future to understand the natural variability of the system and assess potential effects of stressors such as deoxygenation and rising temperature.

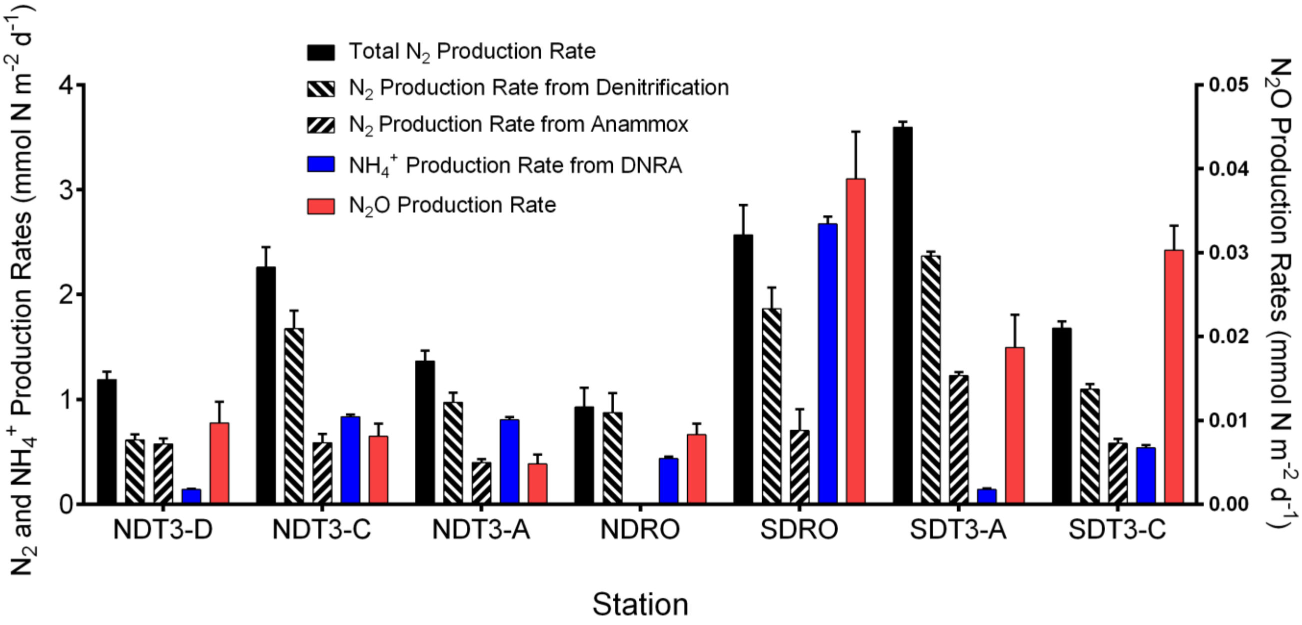

Figure 2. Inorganic N-species production rates determined from $^{15}N\text{-}NO_3^-$ labelling studies with in-situ benthic flux chambers: Production of total N_2, N_2 from denitrification, N_2 from anaerobic ammonia oxidation (anammox), NH_4^+ from dissimilatory nitrate reduction to ammonia (DNRA), and N_2O. Note the lower range (right y-axis) for N_2O production.

N_2 production rates in this study were higher than most of those reported in other studies using in-situ incubations with benthic flux chambers (Bonaglia et al., 2017; De Brabandere et al., 2015; Hall et al., 2017; van Helmond et al., 2020; Hylén et al., 2022). Elevated rates in the SBB are likely a result of the high organic matter content of sediment (4.1 - 6.8% total organic carbon; Table 1), supporting high microbial respiration rates, and little (max. 20 mm) to zero O_2 penetration into the sediment (Yousavich et al., 2023). Compared to the SBB, organic matter content in sediment of previous studies, including the anoxic Eastern Gotland Basin (Hall et al., 2017), the largely pristine and oxygenated Gulf of Bothnia (Bonaglia et al., 2017), and an anoxic fjord basin in the By Fjord on the Swedish west coast (De Brabandere et al., 2015), was lower and the N_2 production rates were typically < 1 mmol N m^{-2} d^{-1}.

https://doi.org/10.5194/egusphere-2023-1498
Preprint. Discussion started: 11 July 2023

In comparison, N_2 production rates reached 1.72 ± 0.77 mmol N m^{-2} d^{-1} in the sediment underlying eutrophic waters of Stockholm archipelago, where organic matter content was similar to SBB sediment (6.3% w/w) and O_2 penetration depth was < 4 mm (van Helmond et al., 2020). Additionally, benthic denitrification rates in the SBB (1.37 ± 0.64 mmol N m^{-2} d^{-1}) were similar to those reported from the Peruvian OMZ (1.31 ± 0.60 mmol N m^{-2} d^{-1}) where bottom water O_2 was lower than 10 µM and the organic matter content was similar (up to 7.5% TOC and 0.9% TON) to that in SBB sediments (Bohlen et al., 2011; Henrichs and Farrington, 1984; Sommer et al., 2016).

Table 2. The relative contribution of different processes (total N_2 production, N_2 from denitrification, N_2 from anammox, NH_4^+ from DNRA, and N_2O Production) to total NO_3^- reduction (upper part) and the relative contribution of total NO_3^- reduction to total NO_3^- uptake (lower part) in the Santa Barbara Basin. Total N_2 production consists of N_2 from denitrification and N_2 from anammox. Total NO_3^- reduction consists of total N_2 production, NH_4^+ from DNRA, and N_2O Production. Total NO_3^- uptake consists of total NO_3^- reduction and other NO_3^- sinks (e.g. intracellular storage).

Processes contributing to Total NO_3^- Reduction	**NDT3-D**	**NDT3-C**	**NDT3-A**	**NDRO**	**SDRO**	**SDT3-A**	**SDT3-C**
Total N_2 Production	85.8%	70.2%	59.2%	66.7%	45.1%	94.9%	71.1%
N_2 from Denitrification	59.2%	60.4%	49.3%	66.7%	38.3%	75.8%	56.8%
N_2 from Anammox	26.6%	9.8%	9.9%	0.0%	6.8%	19.1%	14.3%
NH_4^+ from DNRA	13.3%	29.5%	40.6%	32.7%	54.1%	4.5%	27.3%
N_2O Production	0.9%	0.3%	0.2%	0.6%	0.8%	0.6%	1.5%
Total NO_3^- Reduction	100%	100%	100%	100%	100%	100%	100%
Processes contributing to Total NO_3^- Uptake							
Total NO_3^- Reduction	7.4%	34.5%	16.3%	17.7%	57.7%	16.4%	17.5%
Other NO_3^- Sinks	92.6%	65.5%	83.7%	82.3%	42.3%	83.6%	82.5%
Total NO_3^- uptake	100%	100%	100%	100%	100%	100%	100%

https://doi.org/10.5194/egusphere-2023-1498
Preprint. Discussion started: 11 July 2023

Benthic denitrification rates exceeded anammox rates at all sampling sites (Fig. 2 and Table 2). This relationship agrees with the paradigm that denitrification is typically favored over anammox in organic-rich sediments (Dalsgaard et al., 2005; Devol, 2015). Anammox bacteria can reduce NO_3^- to NO_2^-, which is then used to oxidize ammonia (NH_3) to N_2 (Kartal et al., 2007). In our in-situ incubations, coupled DNRA-anammox in which DNRA produces a substrate (NH_3) required by anammox could result in the production of $^{30}N_2$ (Prokopenko et al., 2006), which is accounted for by our rate calculation method (detailed in section 2.2). However, because the porewater NH_4^+ concentration was high (> 100 µM), the fraction of ^{15}N in the NH_4^+ pool remained low (up to 2.1% after ~1 hour of incubation and up to 4.3% after 6 hours of incubation). Therefore, the contribution of anammox to $^{30}N_2$ production was below 2.0% (Table S3). Overall, anammox contributed up to 26.6% of NO_3^- reduction in the SBB (Table 2), indicating that anammox was a significant process in benthic SBB N cycling. Because the N isotope fractionation during the reduction of nitrite (NO_2^-) to N_2 by anammox bacteria (+16.0 ± 4.5‰) is lower than that of denitrification used for isotope mass balance calculations (~25‰), anammox likely contributed to the lower-than-expected natural abundance ^{15}N enrichment in the SBB water column NO_3^- pool previously measured (Brunner et al., 2013; Sigman et al., 2003). When NO_3^- is not limiting, denitrification typically dominates as the denitrifier population has a shorter generation time than DNRA bacteria (Kraft et al., 2014).

3.3 NO_3^- availability and TOC control the relative importance of DNRA

The contribution of DNRA to total NO_3^- reduction was lower than denitrification at all stations except for the deepest station SDRO (Fig. 2), where NH_4^+ production by DNRA contributed more than half of the NO_3^- reduction (Table 2). The relative contribution of DNRA to total NO_3^- reduction was positively correlated with TOC in the top 2 cm of the sediment (Fig. 3a) and negatively correlated with bottom water NO_3^- concentration (Fig. 3b). These trends are consistent with previous findings showing that DNRA tends to be favored in environments with high availability of electron donors such as organic carbon (Hardison et al., 2015; Kraft et al., 2014; Tiedje et al., 1983) and limited by NO_3^- (van den Berg et al., 2015; Kessler et al., 2018; Peng et al., 2016). Another example where DNRA dominated under limited NO_3^- availability is reported from measurements along a bottom water O_2 and NO_3^- gradient traversing the Peruvian OMZ (Bohlen et al., 2011). One explanation for the increasing importance of DNRA under NO_3^--limited conditions is that the growth yields calculated per mol electron acceptor from DNRA (consumes eight electrons) is higher than from denitrification (consumes five electrons) despite the greater amount of free energy provided by denitrification than DNRA per mol of NO_3^-, which was demonstrated by bacterial cultures capable of denitrification and DNRA (Strohm et al., 2007).

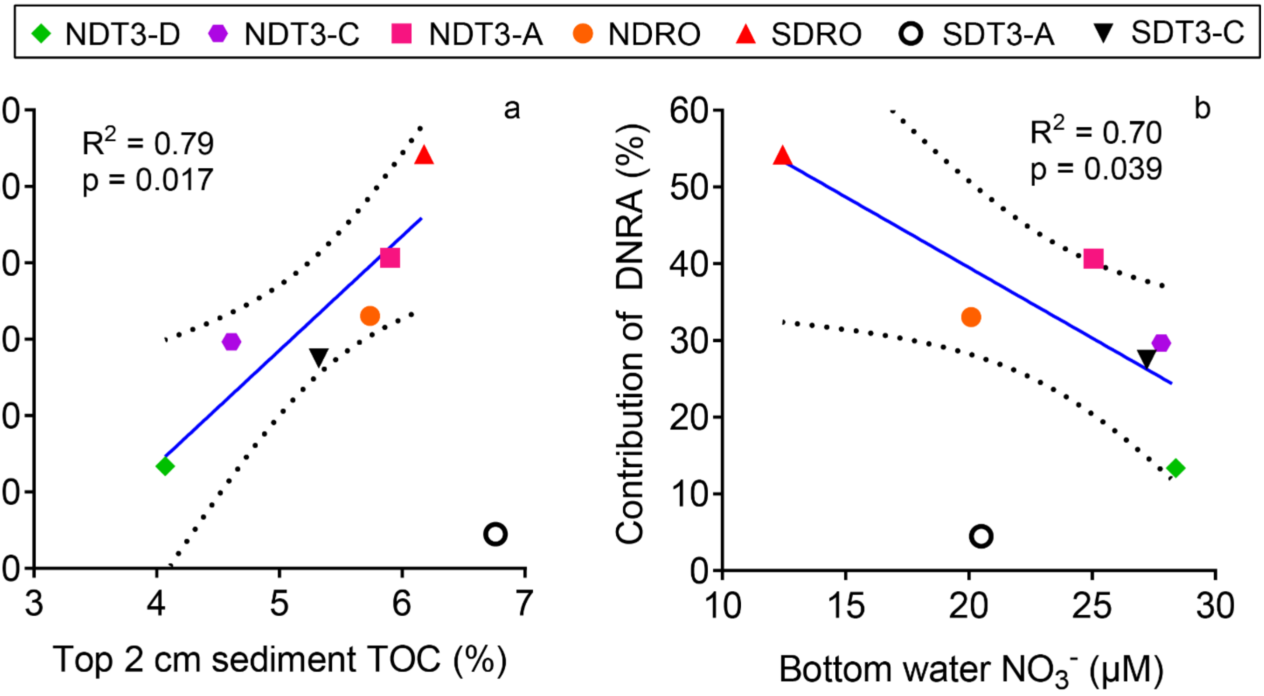

Figure 3. The correlation between the contribution of DNRA to NO_3^- reduction (in %) and **(a)** the C:N ratio of sediment organic matter and **(b)** the bottom water NO_3^- concentration in the Santa Barbara Basin. Linear regressions were performed excluding one outlier from station SDT3-A. The solid line represents the best fit, and the dashed lines represent the 95% confidence interval band.

The regressions we performed between the relative importance of DNRA vs. TOC and bottom water NO_3^- concentration excluded one data point from the station SDT3-A that deviated from the overall trend (Fig. 3). The DNRA rate at SDT3-A (0.14 ± 0.005 mmol N m^{-2} d^{-1}) was similarly low compared to NDT3-D (0.14 ± 0.003 mmol N m^{-2} d^{-1}), but the N_2 production rates by both denitrification and anammox were the highest among all stations (Fig. 2), resulting in the lowest relative importance of DNRA. Porewater sulfide concentration was high at SDT3-A (Yousavich et al., 2023), so the DNRA bacteria should not be limited by the availability of electron donors. Sediments at SDT3-A were characterized by the highest TOC and TON content among all sites (Table 1), which likely fueled the highest rates of denitrification and anammox (Middelburg et al., 1996).

The frequency and magnitude of seasonal anoxia in the SBB has been increasing in the past four decades, which is expected to intensify fixed N loss and NO_3^- deficit in the water column (Goericke et al., 2015). Time-series measurements of water column NO_3^- revealed that bottom water NO_3^- depletion has become more frequent since 2003 compared to the time between 1986 and 2003. While seasonal flushing of the SBB not only oxygenates the bottom water but also increases bottom water NO_3^-, our results suggest that fixed N retention via DNRA will increase in response to NO_3^- drawdown even before NO_3^- is near depletion, which effectively forms negative feedback that could potentially prevent the depletion of fixed N in the SBB. On the other hand, when NO_3^- is no longer limiting, perhaps due to slowdown of bottom water deoxygenation, the relative importance of DNRA would decrease, allowing denitrification to dominate NO_3^- reduction pathways.

3.4 N_2O production and saturation

N_2O production rates measured by in-situ chamber incubations ranged from 4.8 ± 1.1 to 38.8 ± 5.6 μmol m^{-2} d^{-1} (Fig. 2). These rates were up to an order of magnitude higher than those measured using shipboard whole-core incubations (3.5 ± 1.0 μmol m^{-2} d^{-1}) with samples from a similar depth (544 m) in the anoxic part of the Soledad Basin (Townsend-Small et al., 2014). A recent study using in-situ chamber incubations with $^{15}NO_3^-$ in the Eastern Gotland Basin reported rates (~15 - 68 μmol m^{-2} d^{-1}) similar to or higher than the rates we measured in the SBB (Hylén et al., 2022). Because the physicochemical context of the Soledad Basin is more similar to the SBB than the Eastern Gotland Basin, we expected the N_2O production rates in the Soledad Basin to be close to those in the SBB. The much lower N_2O production rates reported from the Soledad Basin may be partially attributed to the whole-core incubations that were not performed in situ.

N_2O production as a fraction of total NO_3^- reduction ranged from 0.2% to 1.5% (Table 2), which fell in the typical range of N_2O yield from both nitrification and denitrification (Ji et al., 2015, 2018). Although our measurements do not allow the distinction between N_2O production from nitrification and denitrification, it is likely that both processes contributed with the respective share depending on ambient O_2 concentration. At the deepest stations where bottom water O_2 was depleted (Table 1), denitrification was likely the main source of N_2O. At other stations, where bottom water O_2 ranged from 3.1 - 9.2 µM, nitrification likely also contributed to N_2O production.

Although we observed N_2O production in all in-situ $^{15}NO_3^-$ incubations, N_2O concentration in the chambers at the start of the incubations was far below saturation level (9 - 12%) at the two deepest stations SDRO and NDRO (Table S4). In contrast, N_2O was either close to or above saturation at all other stations (Table S4). The low concentration of dissolved N_2O at the two deepest stations is consistent with our finding that N_2 production (i.e. N_2O consumption) rates by denitrification were the highest there (Fig. 2), indicating that the deepest part of the SBB typically acts as a sink for N_2O. The shallower parts of the SBB were characterized by a lower NO_3^- uptake rate (Table S2; Fig. S1), but they had a stronger potential for N_2O production than the deepest stations (Fig. S2). In case of a eutrophication event, enhanced surface primary productivity could stimulate denitrification as well as N_2O production in the shallower parts of the SBB where bottom water O_2 is not depleted, where benthic N_2O production is more likely to contribute to N_2O efflux from the water column during upwelling events.

3.5 Total NO_3^- uptake suggests high potential for intracellular NO_3^- storage

Although the N_2 production rates we measured in the SBB were among the highest reported values for any marine sediments, total NO_3^- reduction, which also includes DNRA and N_2O production, only accounted for 23.9 ± 16.9% of the total NO_3^- uptake in benthic flux chambers amended with $^{15}NO_3^-$

https://doi.org/10.5194/egusphere-2023-1498
Preprint. Discussion started: 11 July 2023

(Table 2). Intracellular NO_3^- storage by bacteria and microbial eukaryotes was likely responsible for the majority of the NO_3^- uptake unaccounted for by the different NO_3^- reduction pathways. Marine *Beggiatoa spp.* can hyper-accumulate NO_3^- intracellularly at concentrations 3,000- to 4,000-fold above ambient levels (McHatton et al., 1996). Other microbial lineages including *Thioploca*, foraminifera, and gromiida are also known to store NO_3^- intracellularly (Piña-Ochoa et al., 2010; Zopfi et al., 2001). In two of the porewater profiles sampled during the same cruise, NO_3^- concentrations at 1 cm depth reached 80 - 390 µM, which we interpreted as evidence of NO_3^- leakage from bacterial cells during porewater handling (Yousavich et al., 2023). While it is difficult to directly constrain the contribution of intracellular NO_3^- storage to total NO_3^- uptake, it can be indirectly inferred by calculating the diffusive loss (both upward and downward) of added $^{15}NO_3^-$ if porewater concentrations in sediments underlying the benthic flux chamber were available.

The total NO_3^- uptake in the SBB measured from parallel benthic flux chambers without substrate amendment at the same stations (3.26 ± 0.72 mmol N m^{-2} d^{-1}) (Yousavich et al., 2023) was higher than that in other nearby borderland basins such as the San Nicolas Basin (0.38 ± 0.03 mmol N m^{-2} d^{-1}), the San Pedro Basin (0.78 ± 0.11 mmol N m^{-2} d^{-1}) (Berelson et al., 1987), and the Santa Monica Basin (1.10 ± 0.31 mmol N m^{-2} d^{-1}) (Jahnke, 1990). As mentioned above (section 3.1), the addition of $^{15}NO_3^-$ stimulated NO_3^- uptake rates by multiple folds (compared to BFC incubations without $^{15}NO_3^-$ additions) and to a level (11.60 ± 4.15 mmol N m^{-2} d^{-1}) similar to a previous estimate (11.7 mmol N m^{-2} d^{-1}) based on water column NO_3^- deficit (Valentine et al., 2016). Since bottom water NO_3^- during our sampling time (>12.5 µM in November 2019) was not as depleted as in October 2013 (~2 µM NO_3^-) (Valentine et al., 2016), these results indicate that the microbial community in SBB sediments have the metabolic potential to further consume NO_3^- when SBB bottom water undergoes extended periods (months) of anoxia during autumn and winter. Assuming that NO_3^- in the lowermost 10 m of the water column are under direct influence of benthic NO_3^- uptake, we estimate it would take between one to four months to deplete bottom water NO_3^- with a starting concentration of 30 µM, with the shortest depletion time at the depocenter and the longest at the periphery of the SBB. This timescale agrees with time-series measurements of water-column NO_3^- concentrations in the SBB (Goericke et al., 2015), and it implies that bottom water NO_3^- is unlikely to become depleted at depths shallower than 500 m. Furthermore, we identified a significant negative correlation between NO_3^- uptake rates without substrate amendments and the fold-change after $^{15}NO_3^-$ addition (Fig. S3). This negative correlation indicates that benthic NO_3^- uptake rates at the shallow stations were the most responsive to exogenous NO_3^- supply, while on the other hand NO_3^- uptake rates at the deep and anoxic stations were closer to an upper limit that is determined by the microbial community present in the SBB sediments.

4 Summary

We investigated benthic nitrogen cycling processes using in-situ incubations with $^{15}NO_3^-$ addition and quantified the rates of total NO_3^- uptake, denitrification, anammox, N_2O production, and DNRA. Denitrification was the dominant NO_3^- reduction process (38-76%), while anammox contributed up to 27%. DNRA accounted for less than half of NO_3^- reduction except at the deepest station (586 m), at the center of the SBB, where bottom water O_2 concentrations were zero. The relative importance of DNRA was positively correlated with sediment TOC and negatively correlated with bottom water NO_3^- availability. N_2O production as a fraction of total NO_3^- reduction ranged from 0.2% to 1.5%, which was higher than previous reports from nearby borderland basins. The large fraction of NO_3^- uptake unaccounted for by NO_3^- reduction processes suggests high potential for intracellular storage. Our results indicate the role of the SBB sediments as a strong sink for fixed nitrogen. Future intensification of water column anoxia may elevate the importance of fixed N retention via DNRA by keeping N in the system as NH_4^+, forming negative feedback that could overall reduce fixed N loss in the SBB.

Data availability

The rate data in tabular form are available at https://figshare.com/articles/dataset/Peng_et_al_2023_xlsx/21824610.

Author contribution

XP, TT, and DLV designed the study; XP, DJY, FW, FJ, TT, and DLV participated in the fieldwork; XP, DJY, AB, FW, and FJ performed the measurements; XP wrote the manuscript; All authors contributed to the writing of the manuscript and discussion of the data.

Competing interests

One of the co-authors is a member of the editorial board of Biogeosciences.

Acknowledgements

We thank the captain, crew, and scientific party of the R/V Atlantis, and the crew of the ROV Jason for their technical and logistical support during the research expedition AT42-19. We also thank D. Robinson, S. Krause, Q. Qin, E. Arrington, M. O'Beirne, A. Mazariegos, X. Moreno, A. Eastman, H. Kittner, S. Dorji, J. Burgos-Ponce, N. Liu, J. Tarn, and K. Gosselin for assisting with shipboard analyses. Funding for this work was provided by the US National Science Foundation, NSF OCE-1756947 and OCE-1830033 (to DLV) and OCE-1829981 (to TT), and by a Simons Foundation Postdoctoral Fellowship in Marine Microbial Ecology (No. 547606 to XP).

References

Aller, R. C., Hall, P. O. J., Rude, P. D., and Aller, J. Y.: Biogeochemical heterogeneity and suboxic diagenesis in hemipelagic sediments of the Panama Basin, Deep Sea Research Part I: Oceanographic Research Papers, 45, 133–165, https://doi.org/10.1016/S0967-0637(97)00049-6, 1998.

Becker, J. J., Sandwell, D. T., Smith, W. H. F., Braud, J., Binder, B., Depner, J., Fabre, D., Factor, J., Ingalls, S., Kim, S.-H., Ladner, R., Marks, K., Nelson, S., Pharaoh, A., Trimmer, R., Von Rosenberg, J., Wallace, G., and Weatherall, P.: Global Bathymetry and Elevation Data at 30 Arc Seconds Resolution: SRTM30_PLUS, Marine Geodesy, 32, 355–371, https://doi.org/10.1080/01490410903297766, 2009.

Berelson, W. M., Hammond, D. E., and Johnson, K. S.: Benthic fluxes and the cycling of biogenic silica and carbon in two southern California borderland basins, Geochimica et Cosmochimica Acta, 51, 1345–1363, https://doi.org/10.1016/0016-7037(87)90320-6, 1987.

van den Berg, E. M., van Dongen, U., Abbas, B., and van Loosdrecht, M. C.: Enrichment of DNRA bacteria in a continuous culture, ISME J, 9, 2153–2161, https://doi.org/10.1038/ismej.2015.26, 2015.

Bograd, S. J., Schwing, F. B., Castro, C. G., and Timothy, D. A.: Bottom water renewal in the Santa Barbara Basin, Journal of Geophysical Research: Oceans, 107, 9-1-9–9, https://doi.org/10.1029/2001JC001291, 2002.

Bohlen, L., Dale, A. W., Sommer, S., Mosch, T., Hensen, C., Noffke, A., Scholz, F., and Wallmann, K.: Benthic nitrogen cycling traversing the Peruvian oxygen minimum zone, Geochimica et Cosmochimica Acta, 75, 6094–6111, https://doi.org/10.1016/j.gca.2011.08.010, 2011.

Bonaglia, S., Hylén, A., Rattray, J. E., Kononets, M. Y., Ekeroth, N., Roos, P., Thamdrup, B., Brüchert, V., and Hall, P. O. J.: The fate of fixed nitrogen in marine sediments with low organic loading: an in situ study, Biogeosciences, 14, 285–300, https://doi.org/10.5194/bg-14-285-2017, 2017.

Brunner, B., Contreras, S., Lehmann, M. F., Matantseva, O., Rollog, M., Kalvelage, T., Klockgether, G., Lavik, G., Jetten, M. S. M., Kartal, B., and Kuypers, M. M. M.: Nitrogen isotope effects induced by anammox bacteria, Proceedings of the National Academy of Sciences, 110, 18994–18999, https://doi.org/10.1073/pnas.1310488110, 2013.

Burgin, A. J. and Hamilton, S. K.: Have we overemphasized the role of denitrification in aquatic ecosystems? A review of nitrate removal pathways, Frontiers in Ecology and the Environment, 5, 89–96, https://doi.org/10.1890/1540-9295(2007)5[89:HWOTRO]2.0.CO;2, 2007.

Caffrey, J. M., Bonaglia, S., and Conley, D. J.: Short exposure to oxygen and sulfide alter nitrification, denitrification, and DNRA activity in seasonally hypoxic estuarine sediments, FEMS Microbiology Letters, 366, fny288, https://doi.org/10.1093/femsle/fny288, 2019.

Dalsgaard, T., Thamdrup, B., and Canfield, D. E.: Anaerobic ammonium oxidation (anammox) in the marine environment, Research in Microbiology, 156, 457–464, https://doi.org/10.1016/j.resmic.2005.01.011, 2005.

Dalsgaard, T., Stewart, F. J., Thamdrup, B., Brabandere, L. D., Revsbech, N. P., Ulloa, O., Canfield, D. E., and DeLong, E. F.: Oxygen at Nanomolar Levels Reversibly Suppresses Process Rates and Gene Expression in Anammox and Denitrification in the Oxygen Minimum Zone off Northern Chile, mBio, 5, https://doi.org/10.1128/mBio.01966-14, 2014.

https://doi.org/10.5194/egusphere-2023-1498
Preprint. Discussion started: 11 July 2023

De Brabandere, L., Bonaglia, S., Kononets, M. Y., Viktorsson, L., Stigebrandt, A., Thamdrup, B., and Hall, P. O. J.: Oxygenation of an anoxic fjord basin strongly stimulates benthic denitrification and DNRA, Biogeochemistry, 126, 131–152, https://doi.org/10.1007/s10533-015-0148-6, 2015.

Deming, W. E.: Statistical adjustment of data., 1943.

Devol, A. H.: Denitrification, Anammox, and N2 Production in Marine Sediments, Annual Review of Marine Science, 7, 403–423, https://doi.org/10.1146/annurev-marine-010213-135040, 2015.

Elkins, J. W., Wofsy, S. C., McElroy, M. B., Kolb, C. E., and Kaplan, W. A.: Aquatic sources and sinks for nitrous oxide, Nature, 275, 602–606, https://doi.org/10.1038/275602a0, 1978.

Firestone, M. K., Firestone, R. B., and Tiedje, J. M.: Nitrous Oxide from Soil Denitrification: Factors Controlling Its Biological Production, Science, 208, 749–751, https://doi.org/10.1126/science.208.4445.749, 1980.

García-Robledo, E., Corzo, A., and Papaspyrou, S.: A fast and direct spectrophotometric method for the sequential determination of nitrate and nitrite at low concentrations in small volumes, Marine Chemistry, 162, 30–36, https://doi.org/10.1016/j.marchem.2014.03.002, 2014.

Goericke, R., Bograd, S. J., and Grundle, D. S.: Denitrification and flushing of the Santa Barbara Basin bottom waters, Deep Sea Research Part II: Topical Studies in Oceanography, 112, 53–60, https://doi.org/10.1016/j.dsr2.2014.07.012, 2015.

Gruber, N.: The marine nitrogen cycle: overview and challenges, Nitrogen in the marine environment, 2, 1–50, 2008.

Hall, P. O. J., Brunnegård, J., Hulthe, G., Martin, W. R., Stahl, H., and Tengberg, A.: Dissolved organic matter in abyssal sediments: Core recovery artifacts, Limnology and Oceanography, 52, 19–31, https://doi.org/10.4319/lo.2007.52.1.0019, 2007.

Hall, P. O. J., Almroth Rosell, E., Bonaglia, S., Dale, A. W., Hylén, A., Kononets, M., Nilsson, M., Sommer, S., van de Velde, S., and Viktorsson, L.: Influence of Natural Oxygenation of Baltic Proper Deep Water on Benthic Recycling and Removal of Phosphorus, Nitrogen, Silicon and Carbon, Front. Mar. Sci., 4, https://doi.org/10.3389/fmars.2017.00027, 2017.

Hardison, A. K., Algar, C. K., Giblin, A. E., and Rich, J. J.: Influence of organic carbon and nitrate loading on partitioning between dissimilatory nitrate reduction to ammonium (DNRA) and N2 production, Geochimica et Cosmochimica Acta, 164, 146–160, https://doi.org/10.1016/j.gca.2015.04.049, 2015.

Harris, D., Horwáth, W. R., and van Kessel, C.: Acid fumigation of soils to remove carbonates prior to total organic carbon or CARBON-13 isotopic analysis, Soil Science Society of America Journal, 65, 1853–1856, https://doi.org/10.2136/sssaj2001.1853, 2001.

van Helmond, N. A. G. M., Robertson, E. K., Conley, D. J., Hermans, M., Humborg, C., Kubeneck, L. J., Lenstra, W. K., and Slomp, C. P.: Removal of phosphorus and nitrogen in sediments of the eutrophic Stockholm archipelago, Baltic Sea, Biogeosciences, 17, 2745–2766, https://doi.org/10.5194/bg-17-2745-2020, 2020.

Henrichs, S. M. and Farrington, J. W.: Peru upwelling region sediments near 15°S. 1. Remineralization and accumulation of organic matter1, Limnology and Oceanography, 29, 1–19, https://doi.org/10.4319/lo.1984.29.1.0001, 1984.

Horak, R. E. A., Ruef, W., Ward, B. B., and Devol, A. H.: Expansion of denitrification and anoxia in the eastern tropical North Pacific from 1972 to 2012, Geophys. Res. Lett., 43, 2016GL068871, https://doi.org/10.1002/2016GL068871, 2016.

Hylén, A., Bonaglia, S., Robertson, E., Marzocchi, U., Kononets, M., and Hall, P. O. J.: Enhanced benthic nitrous oxide and ammonium production after natural oxygenation of long-term anoxic sediments, Limnology and Oceanography, 67, 419–433, https://doi.org/10.1002/lno.12001, 2022.

Jahnke, R. A.: Early diagenesis and recycling of biogenic debris at the seafloor, Santa Monica Basin, California, Journal of Marine Research, 48, 413–436, https://doi.org/10.1357/002224090784988773, 1990.

Ji, Q., Babbin, A. R., Jayakumar, A., Oleynik, S., and Ward, B. B.: Nitrous oxide production by nitrification and denitrification in the Eastern Tropical South Pacific oxygen minimum zone, Geophysical Research Letters, 42, 10,755-10,764, https://doi.org/10.1002/2015GL066853, 2015.

Ji, Q., Buitenhuis, E., Suntharalingam, P., Sarmiento, J. L., and Ward, B. B.: Global Nitrous Oxide Production Determined by Oxygen Sensitivity of Nitrification and Denitrification, Global Biogeochemical Cycles, 32, 1790–1802, https://doi.org/10.1029/2018GB005887, 2018.

Joye, S. B. and Hollibaugh, J. T.: Influence of Sulfide Inhibition of Nitrification on Nitrogen Regeneration in Sediments, Science, 270, 623–625, https://doi.org/10.1126/science.270.5236.623, 1995.

Kartal, B., Kuypers, M. M. M., Lavik, G., Schalk, J., Op den Camp, H. J. M., Jetten, M. S. M., and Strous, M.: Anammox bacteria disguised as denitrifiers: nitrate reduction to dinitrogen gas via nitrite and ammonium, Environmental Microbiology, 9, 635–642, https://doi.org/10.1111/j.1462-2920.2006.01183.x, 2007.

Kessler, A. J., Roberts, K. L., Bissett, A., and Cook, P. L. M.: Biogeochemical Controls on the Relative Importance of Denitrification and Dissimilatory Nitrate Reduction to Ammonium in Estuaries, Global Biogeochemical Cycles, 32, 1045–1057, https://doi.org/10.1029/2018GB005908, 2018.

Kononets, M., Tengberg, A., Nilsson, M., Ekeroth, N., Hylén, A., Robertson, E. K., van de Velde, S., Bonaglia, S., Rütting, T., Blomqvist, S., and Hall, P. O. J.: In situ incubations with the Gothenburg benthic chamber landers: Applications and quality control, Journal of Marine Systems, 214, 103475, https://doi.org/10.1016/j.jmarsys.2020.103475, 2021.

Koslow, J., Goericke, R., McClatchie, S., Vetter, R., and Rogers-Bennett, L.: The California Cooperative Oceanic Fisheries Investigations (CalCOFI): the continuing evolution and contributions of a 60-year ocean observation program, 2010.

Kraft, B., Tegetmeyer, H. E., Sharma, R., Klotz, M. G., Ferdelman, T. G., Hettich, R. L., Geelhoed, J. S., and Strous, M.: The environmental controls that govern the end product of bacterial nitrate respiration, Science, 345, 676–679, https://doi.org/10.1126/science.1254070, 2014.

Laima, M. C. J.: Is KCl a reliable extractant of15NH4+added to coastal marine sediments?, Biogeochemistry, 27, 83–95, https://doi.org/10.1007/BF00002812, 1994.

McHatton, S. C., Barry, J. P., Jannasch, H. W., and Nelson, D. C.: High Nitrate Concentrations in Vacuolate, Autotrophic Marine Beggiatoa spp, Applied and Environmental Microbiology, 62, 954–958, https://doi.org/10.1128/aem.62.3.954-958.1996, 1996.

McIlvin, M. R. and Altabet, M. A.: Chemical Conversion of Nitrate and Nitrite to Nitrous Oxide for Nitrogen and Oxygen Isotopic Analysis in Freshwater and Seawater, Anal. Chem., 77, 5589–5595, https://doi.org/10.1021/ac050528s, 2005.

Middelburg, J. J., Soetaert, K., Herman, P. M. J., and Heip, C. H. R.: Denitrification in marine sediments: A model study, Global Biogeochemical Cycles, 10, 661–673, https://doi.org/10.1029/96GB02562, 1996.

Myhre, S. E., Pak, D., Borreggine, M., Kennett, J. P., Nicholson, C., Hill, T. M., and Deutsch, C.: Oxygen minimum zone biotic baseline transects for paleoceanographic reconstructions in Santa Barbara Basin, CA, Deep Sea Research Part II: Topical Studies in Oceanography, 150, 118–131, https://doi.org/10.1016/j.dsr2.2017.12.009, 2018.

Nielsen, L. P. and Glud, R. N.: Denitrification in a coastal sediment measured in situ by the nitrogen isotope pairing technique applied to a benthic flux chamber, Marine Ecology Progress Series, 137, 181–186, https://doi.org/10.3354/meps137181, 1996.

Oschlies, A., Duteil, O., Getzlaff, J., Koeve, W., Landolfi, A., and Schmidtko, S.: Patterns of deoxygenation: sensitivity to natural and anthropogenic drivers, Philosophical Transactions of the Royal Society A: Mathematical, Physical and Engineering Sciences, 375, 20160325, https://doi.org/10.1098/rsta.2016.0325, 2017.

Paulmier, A. and Ruiz-Pino, D.: Oxygen minimum zones (OMZs) in the modern ocean, Progress in Oceanography, 80, 113–128, https://doi.org/10.1016/j.pocean.2008.08.001, 2009.

Peng, X., Ji, Q., Angell, J. H., Kearns, P. J., Yang, H. J., Bowen, J. L., and Ward, B. B.: Long-term fertilization alters the relative importance of nitrate reduction pathways in salt marsh sediments, J. Geophys. Res. Biogeosci., 2016JG003484, https://doi.org/10.1002/2016JG003484, 2016.

Piña-Ochoa, E., Høgslund, S., Geslin, E., Cedhagen, T., Revsbech, N. P., Nielsen, L. P., Schweizer, M., Jorissen, F., Rysgaard, S., and Risgaard-Petersen, N.: Widespread occurrence of nitrate storage and denitrification among Foraminifera and Gromiida, Proceedings of the National Academy of Sciences, 107, 1148–1153, https://doi.org/10.1073/pnas.0908440107, 2010.

Prokopenko, M. G., Hammond, D. E., Berelson, W. M., Bernhard, J. M., Stott, L., and Douglas, R.: Nitrogen cycling in the sediments of Santa Barbara basin and Eastern Subtropical North Pacific: Nitrogen isotopes, diagenesis and possible chemosymbiosis between two lithotrophs (Thioploca and Anammox)—"riding on a glider," Earth and Planetary Science Letters, 242, 186–204, https://doi.org/10.1016/j.epsl.2005.11.044, 2006.

Qin, Q., Kinnaman, F. S., Gosselin, K. M., Liu, N., Treude, T., and Valentine, D. L.: Seasonality of water column methane oxidation and deoxygenation in a dynamic marine environment, Geochimica et Cosmochimica Acta, 336, 219–230, https://doi.org/10.1016/j.gca.2022.09.017, 2022.

Reimers, C. E., Lange, C. B., Tabak, M., and Bernhard, J. M.: Seasonal spillover and varve formation in the Santa Barbara Basin, California, Limnology and Oceanography, 35, 1577–1585, https://doi.org/10.4319/lo.1990.35.7.1577, 1990.

Robertson, E. K., Bartoli, M., Brüchert, V., Dalsgaard, T., Hall, P. O. J., Hellemann, D., Hietanen, S., Zilius, M., and Conley, D. J.: Application of the isotope pairing technique in sediments: Use, challenges, and new directions, Limnology and Oceanography: Methods, 17, 112–136, https://doi.org/10.1002/lom3.10303, 2019.

Schlitzer, R.: Interactive analysis and visualization of geoscience data with Ocean Data View, Computers & Geosciences, 28, 1211–1218, https://doi.org/10.1016/S0098-3004(02)00040-7, 2002.

Shao, M.-F., Zhang, T., Fang, H. H.-P., and Li, X.: The effect of nitrate concentration on sulfide-driven autotrophic denitrification in marine sediment, Chemosphere, 83, 1–6, https://doi.org/10.1016/j.chemosphere.2011.01.042, 2011.

Sholkovitz, E. R. and Gieskes, J. M.: A Physical-Chemical Study of the Flushing of the Santa Barbara Basin1, Limnology and Oceanography, 16, 479–489, https://doi.org/10.4319/lo.1971.16.3.0479, 1971.

Sigman, D. M., Robinson, R., Knapp, A. N., van Geen, A., McCorkle, D. C., Brandes, J. A., and Thunell, R. C.: Distinguishing between water column and sedimentary denitrification in the Santa Barbara Basin using the stable isotopes of nitrate, Geochemistry, Geophysics, Geosystems, 4, https://doi.org/10.1029/2002GC000384, 2003.

Sommer, S., Gier, J., Treude, T., Lomnitz, U., Dengler, M., Cardich, J., and Dale, A. W.: Depletion of oxygen, nitrate and nitrite in the Peruvian oxygen minimum zone cause an imbalance of benthic nitrogen fluxes, Deep Sea Research Part I: Oceanographic Research Papers, 112, 113–122, https://doi.org/10.1016/j.dsr.2016.03.001, 2016.

Stevens, E. D.: Use of plastic materials in oxygen-measuring systems, Journal of Applied Physiology, 72, 801–804, https://doi.org/10.1152/jappl.1992.72.2.801, 1992.

Stramma, L., Johnson, G. C., Sprintall, J., and Mohrholz, V.: Expanding Oxygen-Minimum Zones in the Tropical Oceans, Science, 320, 655–658, https://doi.org/10.1126/science.1153847, 2008.

Strohm, T. O., Griffin, B., Zumft, W. G., and Schink, B.: Growth Yields in Bacterial Denitrification and Nitrate Ammonification, Applied and Environmental Microbiology, 73, 1420–1424, https://doi.org/10.1128/AEM.02508-06, 2007.

Thamdrup, B. and Dalsgaard, T.: Production of N2 through Anaerobic Ammonium Oxidation Coupled to Nitrate Reduction in Marine Sediments, Appl. Environ. Microbiol., 68, 1312–1318, https://doi.org/10.1128/AEM.68.3.1312-1318.2002, 2002.

Thunell, R. C.: Particle fluxes in a coastal upwelling zone: sediment trap results from Santa Barbara Basin, California, Deep Sea Research Part II: Topical Studies in Oceanography, 45, 1863–1884, https://doi.org/10.1016/S0967-0645(98)80020-9, 1998.

Tiedje, J. M., Sexstone, A. J., Myrold, D. D., and Robinson, J. A.: Denitrification: ecological niches, competition and survival, Antonie van Leeuwenhoek, 48, 569–583, https://doi.org/10.1007/BF00399542, 1983.

Townsend-Small, A., Prokopenko, M. G., and Berelson, W. M.: Nitrous oxide cycling in the water column and sediments of the oxygen minimum zone, eastern subtropical North Pacific, Southern California, and Northern Mexico (23°N–34°N), Journal of Geophysical Research: Oceans, 119, 3158–3170, https://doi.org/10.1002/2013JC009580, 2014.

Valentine, D. L., Fisher, G. B., Pizarro, O., Kaiser, C. L., Yoerger, D., Breier, J. A., and Tarn, J.: Autonomous Marine Robotic Technology Reveals an Expansive Benthic Bacterial Community Relevant to Regional Nitrogen Biogeochemistry, Environ. Sci. Technol., 50, 11057–11065, https://doi.org/10.1021/acs.est.6b03584, 2016.

Vonnahme, T. R., Molari, M., Janssen, F., Wenzhöfer, F., Haeckel, M., Titschack, J., and Boetius, A.: Effects of a deep-sea mining experiment on seafloor microbial communities and functions after 26 years, Science Advances, 6, eaaz5922, https://doi.org/10.1126/sciadv.aaz5922, 2020.

Yousavich, D. J., Robinson, D., Peng, X., Krause, S. J. E., Wenzhoefer, F., Janßen, F., Liu, N., Tarn, J., Kinnaman, F., Valentine, D. L., and Treude, T.: Marine anoxia initiates giant sulfur-bacteria mat proliferation and associated changes in benthic nitrogen, sulfur, and iron cycling in the Santa Barbara Basin, California Borderland, EGUsphere, 1–48, https://doi.org/10.5194/egusphere-2023-1198, 2023.

Zehr, J. P.: New twist on nitrogen cycling in oceanic oxygen minimum zones, Proceedings of the National Academy of Sciences, 106, 4575–4576, https://doi.org/10.1073/pnas.0901266106, 2009.

Zhang, L., Altabet, M. A., Wu, T., and Hadas, O.: Sensitive Measurement of NH4+ 15N/14N (δ15NH4+) at Natural Abundance Levels in Fresh and Saltwaters, Anal. Chem., 79, 5297–5303, https://doi.org/10.1021/ac070106d, 2007.

Zopfi, J., Kjær, T., Nielsen, L. P., and Jørgensen, B. B.: Ecology of Thioploca spp.: Nitrate and Sulfur Storage in Relation to Chemical Microgradients and Influence ofThioploca spp. on the Sedimentary Nitrogen Cycle, Applied and Environmental Microbiology, 67, 5530–5537, https://doi.org/10.1128/AEM.67.12.5530-5537.2001, 2001.

Zumft, W. G.: Cell biology and molecular basis of denitrification., Microbiol. Mol. Biol. Rev., 61, 533–616, 1997.